# Development of a handheld thermal neutron detector (GAMBE) using stacked silicon sensors coated with $^6$LiF films

A. Ahmed[a,b,*], S. Burdin[b,*], G. Casse[b], H. van Zalinge[c], S. Powel[b], J. Rees[b], A. Smith[b], I. Tsurin[b]

[a] *Military Technical College, Department of Nuclear Engineering, Cairo, Egypt*
[b] *University of Liverpool, Department of Physics, Liverpool, UK, L69 7ZE*
[c] *University of Liverpool, Department of Electrical Engineering and Electronics, Liverpool, UK, L69 3GJ*

## Abstract

Thermal neutron detectors, which are based on semiconductor material such as silicon coated with neutron reactive material like $^6$LiF have been discussed for many decades. The performance of the thermal neutron detector system, GAMBE (GAMma Blind neutron Efficient), which is based on two silicon sensors in a sandwich configuration is investigated. This detector is able to achieve a total and a coincidence detection efficiency of 4% and ∼1% respectively. The thermal neutron detection efficiency of the detector is enhanced by using a stacked detector configuration and high-density polyethylene (HDPE) sheets, as neutron moderators and reflectors. The GAMBE detector is positioned inside a box of HDPE with a lead window in the direction of the neutron flux for neutron moderation and a reduction of the effect of gamma-rays on the detector. The experimental layout was modeled in MCNP4C to investigate the contribution of HDPE to the thermal neutron flux (n/s/cm$^2$). In this research a stack of 4 silicon semiconductor sensors with (2.6±0.6) and (2.9±0.6) mg/cm$^2$ thick $^6$LiF film in a configuration of two sandwiches is shown to achieve a total and a coincidence detection efficiency of 27% and 4% respectively. This represents a significant improvement compared to a single detector. The effect of these stacked detectors for the development of a handheld thermal neutron detector, using 4 coated Si detectors is shown to have a 22% efficiency. This information is used to inform the optimised design of the handheld detector. The results based on geant4 and MCNP simulations indicate that the total detection efficiency of this portable detector with a stack of 7 sandwich detectors will increase up to 52% by using an optimal thickness of $^6$LiF of 3.95 mg/cm$^2$.

*Keywords:* solid state neutron detectors, neutron detector, coated semiconductor detector, neutron detection, neutron conversion.

## 1. Introduction

Detection of neutrons has become a prime importance in today's world owing to the huge destruction capabilities and security threats [1]. Neutron detectors can indicate the presence of a nuclear explosive device or special nuclear material (SNM) such as plutonium, which could be used to build one [2]. In the past, $^3$He-gas filled proportional counters were most commonly used for thermal neutron detection due to their high detection efficiency (> 60%) and insensitivity to gamma radiation [3–5]. Recently there has been great interest in alternative detection technologies motivated by the shortage of $^3$He and, thus, an inability to produce more $^3$He gas tube thermal neutron detectors. Included among these different alternative neutron detection technologies are solid state neutron detectors that incorporate a semiconductor material such as silicon in their design. These detectors must be adapted in order to be used for thermal neutron detection. They have to be coupled with a suitable neutron converter material, preferably in the form of a converter film/foil, whose capture products are charged particles, which are able to reach the sensitive volume of the detector. This converter material should have a high thermal neutron absorption cross section ($\sigma$) and low atomic density, which improves the range of the charged particles through the converter film or foil. One of the most studied material as a neutron converter is $^6$Li [6–9].

$^6$Li has a thermal neutron absorption cross section ($\sigma$) 940 b, which is affected by neutron energy as it decreases by increasing neutron kinetic energy [10]. It has been demonstrated that the primary reaction of the interacted neutron with $^6$Li is $^6$Li(n,$\alpha$)$^3$H; this reaction produces an alpha particle (at 2.05 MeV) and a triton (at 2.73 MeV) in opposite directions, where the total amount of energy released (Q-value) per reaction is 4.78 MeV [11, 12]. Although $^6$Li has a smaller thermal neutron absorption cross section than $^{10}$B, the higher energy reaction products and lower atomic mass density of $^6$Li make it attractive to be used as a converter film/foil for thermal neutron detectors. This is due to the higher range of reaction products through a $^6$Li converter than that inside a $^{10}$B. $^6$Li results in an improved range of the reaction products through the converter film/foil, where the efficient range of a triton ($L_t$) and an alpha-particle ($L_\alpha$) in a converter foil is 126.77 and 19.05 $\mu$m respectively. Furthermore, It can be used in the stable form of $^6$LiF, however, the range of reaction products will be affected with $L_t$ = 29.25 $\mu$m and $L_\alpha$ = 4.64 $\mu$m [6–9].

In the present work, the performance of the thermal neutron

*Corresponding authors
*Email addresses:* a.ahmed5884@gmail.com (A. Ahmed ), s.burdin@liv.ac.uk (S. Burdin )

detection system, GAMBE, which is based on two silicon sensors and a layer of $^6$LiF as a neutron sensitive material in a sandwich configuration is investigated. The basic design consideration of this sandwich detector configuration is studied using Geant4 simulations [13] to identify the optimal thickness of a $^6$LiF film to achieve the highest total and coincidence detection efficiency. Tests are performed using an $^{241}$Am-$^9$Be neutron source in order to verify the accuracy of the simulation. In addition, HDPE sheets have been used to encircle the detector to examine their effect on the neutron flux distribution and the detector detection efficiency. MCNP-4C code [14] has been used to perform an evaluation of the neutron flux distribution due to the effect of the HDPE sheets. These simulations have been verified by the determination of the enhancement of the total and coincidence detection efficiency of the detector, GAMBE, using a combination between the HDPE sheets and a stacked design of the sandwich detector configuration with a $^6$LiF reactive film. This information has ultimately been combined to suggest an optimum configuration for a handheld thermal neutron detector.

## 2. Detector performance

### 2.1. Planar semiconductor detector in a sandwich design

Planar designs are the most straight forward adaptation of semiconductor detectors for neutron detection. However, they have their limitation. Firstly, the probability of neutron capture in the converter increases with increasing layer thickness. On the other hand, the chance that the neutron capture reaction products will reach the detectors sensitive part decreases with the growth of the neutron converter thickness. Therefore, an optimal converter thickness of the $^6$LiF material has to be found. Secondly, only those charged particles which are ejected in the direction of the sensor interface will be detected. This is known as $2\pi$ geometry which allows only up to half of the primary reaction products to generate e−h pairs inside the depletion region of the semiconductor detector. However, sandwich stacking will lead to $4\pi$ collection of primary reaction products; as the detection of both primary reaction products becomes possible and this increases the thermal neutron detection efficiency.

For GAMBE, the charge sensitive part is a Si diode which has a p-n junction configuration. The bulk is p-type Si semiconductor 300 $\mu$m thick, where its surface is doped by phosphorous ion implantation to form a n$^+$ region of 200 nm thickness. Geant4 simulations were performed to predict the optimal $^6$LiF film thickness where neutron detection efficiency is the highest using a sandwich configuration of two silicon diodes. The thermal neutron detection efficiency, $\varepsilon_n$, of this sandwich detector can be derived from the product of two probabilities as shown in eq. (1). The first is the detection probability of the charged particle reaction products, $\varepsilon_{det} = \frac{n}{N}$, which is defined as the ratio of the detected charged particles ($n$) by the Si sensors to the number of captured neutrons ($N$) within the converter volume. This ratio is affected by the solid angles of these charged particles via the converter layer towards the silicon sensors and the converter thickness, x. The second is the neutron capture probability, $\varepsilon_{abs} = 1-P(x)$, within the converter film as a function of its thickness, where $P(x)$ is the neutron escape probability [15].

$$\varepsilon_n = \varepsilon_{det} \times \varepsilon_{abs} = \frac{n}{N} \times \{1 - P(x)\} \tag{1}$$

The absorption probability $\varepsilon_{abs}$ is proportional to the initial neutron flux ($I_\circ$) through the thickness of the neutron converter. The transmitted neutron flux ($I_x$) through thickness, $x$, is described by

$$I_x = I_\circ \times P(x) = I_\circ \times exp(-\frac{N_A}{w_A} \times \rho \times \sigma \times x), \tag{2}$$

where $N_A$ is Avogadro's number, $w_A$ the atomic or molecular weight of the reactive film/foil, $\rho$ the density of the reactive film/foil and $\sigma$ is the thermal-neutron absorption cross-section of $^6$Li, 940 b. It is clear that the fraction of neutrons passing through the converter layer of thickness, $x$, without any interaction is

$$P(x) = \frac{I_x}{I_\circ} = exp(-\frac{N_A}{w_A} \times \rho \times \sigma \times x). \tag{3}$$

Therefore, the second term in eq. (1) of the thermal neutron detection efficiency, which represents the absorption probability, $\varepsilon_{abs}$, as a function of the converter thickness, $x$, is defined as following

$$\varepsilon_{abs} = 1 - P(x) = 1 - exp(-\frac{N_A}{w_A} \times \rho \times \sigma \times x). \tag{4}$$

Finally, the thermal neutron detection efficiency, $\varepsilon_n$, of the detector is determined using eq. (5), as follows.

$$\varepsilon_n = \frac{n}{N} \times \{1 - exp(-\frac{N_A}{w_A} \times \rho \times \sigma \times x)\} \tag{5}$$

A neutron is counted by detecting either an alpha or a triton as a single or/and a coincident event. This is defined as the total detection efficiency of the detector ($\varepsilon_{tn}$). Detecting neutron capture products in coincidence is a method based on detection of both reaction products (alpha and triton) by two Si sensors and, thus, the coincidence detection efficiency ($\varepsilon_{cn}$) of the detector can be defined. These coincidences provide a very good method for rejecting the spurious hits coming from gamma-ray, which are usually present in a neutron field. However, the price to pay is a reduction of the thermal neutron detection efficiency of the detector.

The detection efficiency depends on both the probability that a neutron can be captured and the chance that secondary particles created in the $^6$LiF film will be capable of reaching the sensitive detector volume. Therefore, the total and coincidence detection efficiency increases up to a certain value of a $^6$LiF film thickness after which they will decrease. The results obtained from the simulations indicate that the optimal film thicknesses for the highest total and coincidence detection efficiency of 7.5% and 1.1% are 8.14 and 1.16 mg/cm$^2$ respectively as presented in fig. 1.

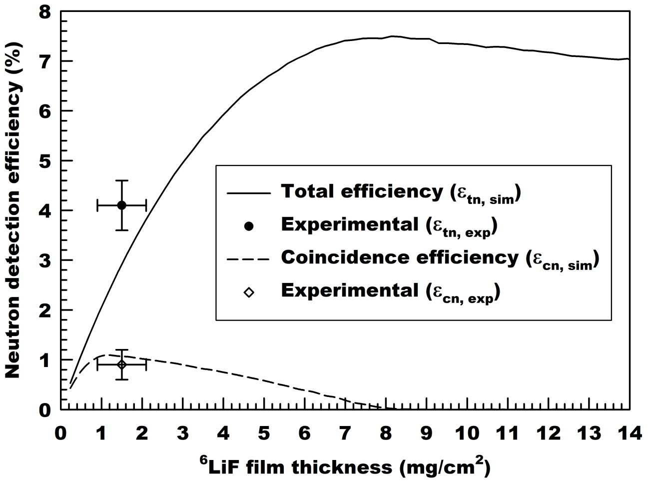


Figure 1: Variation of thermal neutron detection efficiency as a function of $^{6}$LiF film thickness corresponding to one sandwich configuration. In addition to the experimental results of the detector with $^{6}$LiF film (1.5±0.6) mg/cm$^2$ thick.

### 2.2. *Experimental setup and measurements*

#### 2.2.1. *Neutrons source characterisation and flux measurement*

The source of neutrons used for all experiments is a 1 Ci $^{241}$Am-$^{9}$Be neutron source. Neutrons are emitted as part of the reaction:

$$^{9}_{3}\mathrm{Be} + ^{4}_{2}\mathrm{He} \longrightarrow ^{12}_{6}\mathrm{C} + ^{1}_{0}\mathrm{n} + \gamma$$

the total neutron emission rate of a 1 Ci $^{241}$Am-$^{9}$Be neutron source is $2.5 \times 10^6$ neutrons per second (n/s). The reaction Be($\alpha$,n)C$^*$ will often lead to the emission of 4.43 MeV $\gamma$-rays from the excited carbon nucleus. These $\gamma$-rays are produced at a ratio of 0.6:1 $\gamma/n$ [16]. Moreover, $^{241}$Am is not only an $\alpha$ emitter but it also emits $\gamma$-rays of 26, 33 and 60 keV as a part of the following decay reaction.

$$^{241}\mathrm{Am} \longrightarrow ^{237}\mathrm{Np}^* + \alpha$$

$$^{237}\mathrm{Np}^* \longrightarrow ^{237}\mathrm{Np} + \gamma$$

This is in addition to 2.26 MeV $\gamma$-rays, which are emitted as a result of radiative capture reaction where neutrons interact with hydrogenous moderating materials (water in this case).

$$^{1}_{0}\mathrm{n} + ^{1}_{1}\mathrm{H} \longrightarrow ^{2}_{1}\mathrm{H} + \gamma$$

Therefore, it is necessary for all experimental measurements to take into consideration the deposition of energy related to $\gamma$-rays in the silicon sensors of the neutron detector.

The thermal neutron flux has been measured using a $^{3}$He detector tube. The tube is 50 cm away from the end of the neutron tank, and the 1 Ci $^{241}$Am-$^{9}$Be neutron source is 25 cm inside a water tank. This position is referred to as the calibration position where the detector will be tested, and the whole setup is defined as the "Basic" layout. The $^{3}$He detector tubes are industry standard 2 in. (5 cm) diameter, 36 in. active length tubes (90 cm), a pressure of 2 atm, and operating at a voltage of 1100 V. The typical thermal neutron detection efficiency of these $^{3}$He detector tubes is > 60%. Furthermore, the neutron sensitivity of these detectors is 236 cps/*nv* (*nv* is thermal neutron flux, neutrons/cm$^2$/s). This equals to approximately 3 cps/*nv* per cm active tube length assuming no degradation of performance over the lifetime of the detector.

#### 2.2.2. *Gamma-ray rejection factor*

Two bare silicon sensors with an active area of $1 \times 1$ cm$^2$ have been used in a sandwich configuration without any neutron converter material to count events as a result of gamma-ray interaction with the sensors resembling a thermal neutron. Two different gamma ray sources have been used to characterise the sensitivity of the detector to gamma radiation, which is needed to estimate the $\gamma$-ray rejection factor. The bare detector has been examined using the $^{241}$Am-$^{9}$Be neutron source where the detector was placed in the calibration position as defined before. In addition, the detector has been tested by placing it 2 cm in front of a $^{60}$Co gamma-ray source with an activity of 30 kBq. These measurements are used in the calculation of the gamma rejection factor based on the efficiency of the bare detector to detect gamma photons.

Gamma-ray detection efficiency depends on the energy of the incident photon and the thickness of the silicon wafer. The sensitivity of Si sensors to high energy gamma-rays is expected to be low for a thickness range of 30−300 $\mu$m. In particular, a silicon sensor of 300 $\mu$m thickness has a detection efficiency of nearly 100% for $\gamma$-ray energy of 10 keV, falling to 1% for 150 keV [17]. Thus, a Si sensor with a thickness of 300 $\mu$m is compatible with a high background gamma rays. Also, this thickness is optimal to reduce electronic noise as the capacitance decreases as the thickness of the depletion region increases up to 300 $\mu$m corresponding to a fully depleted diode at a voltage of 80 V.

The gamma-ray rejection factor of the detector is determined based on the measurements using a $^{60}$Co gamma-ray source, where 597 photons hit the detector per second, according to the geometrical efficiency. The rejection of background gamma-ray depends on the deposited energy in the detector due to the interaction of gamma-ray with the sensitive volume of the Si sensors of GAMBE. From fig. 2, it is apparent that the rejection factor of background gamma radiation ($\gamma_{rf}$) and the detection efficiency ($\varepsilon_{t\gamma}$ or $\varepsilon_{c\gamma}$) are affected by the variation of the applied PHD method. This figure also shows that the gamma-ray detection efficiency is severely reduced, as any contribution from gamma-ray will be rejected, when the PHD energy is greater than 0.75 MeV. Thus, GAMBE can achieve a high gamma-ray rejection factor of $10^8$, so it could be used efficiently for the detection of thermal neutrons in a high background gamma radiation field.

#### 2.2.3. *Si sensor coated with $^{6}$LiF film*

A $^{6}$LiF solution was prepared by dissolving 3 g of ball milled $^{6}$LiF powder (Sigma-Aldrich 95% enriched $^{6}$Li) in 20 cc ethanol. The $^{6}$LiF solution was mixed with a ratio (*r*) of 1:1 with a solution of 1% polyvinylpyrrolidone (Sigma-Aldrich PVP, MW 700000) in ethanol , which is used as an adhesive material. This mixture of $^{6}$LiF/PVP was precipitated on the

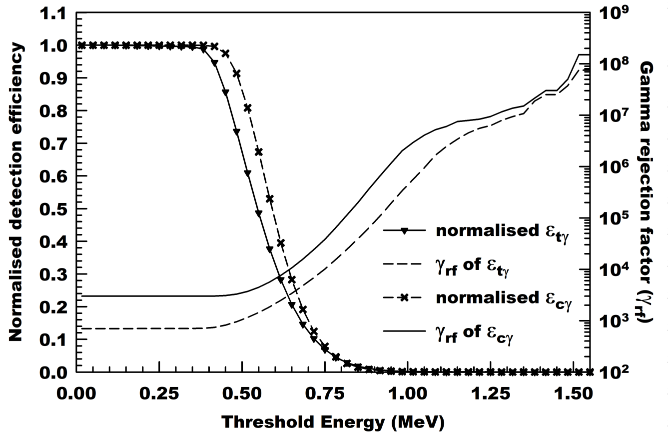


Figure 2: Variation of gamma-ray detection efficiency and the corresponding gamma-ray rejection factor as a function of the threshold energy.

surface of the Si sensor (total area of $1.25 \times 1.25$ cm$^2$). The precipitated mixture was dried at room temperature to avoid cracks and to form a uniform film over the area of the Si substrate. The mass of $^6$LiF/PVP solution to be poured on Si sensor substrate is determined based on the required $^6$LiF film thickness. The mass of the poured solution was measured by a balance. In order to characterise the surface roughness of the deposited films, an atomic force microscope (AFM) was used. It was found that the precipitated films of $^6$LiF on the silicon sensors have a surface roughness of 5 $\mu$m. This results in an error in the mass distribution of ± 0.6 mg/cm$^2$ over the whole area of the formed $^6$LiF films.

#### 2.2.4. *GAMBE detection efficiency validation*

Experimental measurements have been performed using a $^6$LiF film (1.5±0.6) mg/cm$^2$ thick in a sandwich configuration. The entire sensor-converter configuration was mounted in an aluminium box (inner dimension 60 mm × 50 mm × 30 mm) designed to eliminate photoelectric noise, with the coated Si sensor facing the neutron source. These measurements have been accomplished to examine the thermal neutron detection efficiency of the detector at the calibration position related to the “Basic” layout experiment.

The detection efficiency of the detector is assessed after subtracting all events belonging to gamma-ray interaction within the detector, both single and coincidence events. This contribution affects the count rate especially in the low energy range where there is a possibility of interference between the interactions of $\alpha$-particles and $\gamma$-rays with the depleted region of silicon sensor (sensitive volume for the charged particles). However, this step ensures that the evaluated detection efficiency is an absolute thermal neutron detection efficiency. Consequently, a $^6$LiF film of (1.5±0.6) mg/cm$^2$ thick in a sandwich detector configuration can achieve a total and a coincidence detection efficiency of (4.1±0.5)% and (0.9±0.3)% respectively (see fig. 1). These results are in agreement with the expected performance of the detector from the theoretical investigation.

## 3. Contribution of HDPE to detection efficiency

### 3.1. *Monte Carlo simulation of neutron flux*

Monte Carlo N-Particle transport code (MCNP) simulations were performed to have a full depiction of the total ($\Phi_{t,sim}$) and the thermal ($\Phi_{th,sim}$) neutron flux (n/cm$^2$/s) through an area of 1 cm$^2$ of $^6$LiF film. In these simulations, the geometry of two different experimental layouts are modeled, where an isotropic $^{241}$Am-$^9$Be neutron source generating $1.5\times10^9$ particles with energies up to 11 MeV is assumed. In the first simulation labeled as the “Basic” layout, the detector is in line with the neutron source, 75 cm away including 25 cm of water. The detector is without any surrounding physical experimental material such as HDPE sheets or lead blocks. In the second simulation, “HDPE” layout, the detector is in the same position as the first layout, but enclosed by 4 sheets of HDPE. Each sheet is 2 cm thick and has an area of 60 cm × 60 cm. The detector in the second layout is also shielded by lead blocks of 5 cm thickness in the direction of the neutron flux for gamma-ray suppression as depicted in fig. 3.

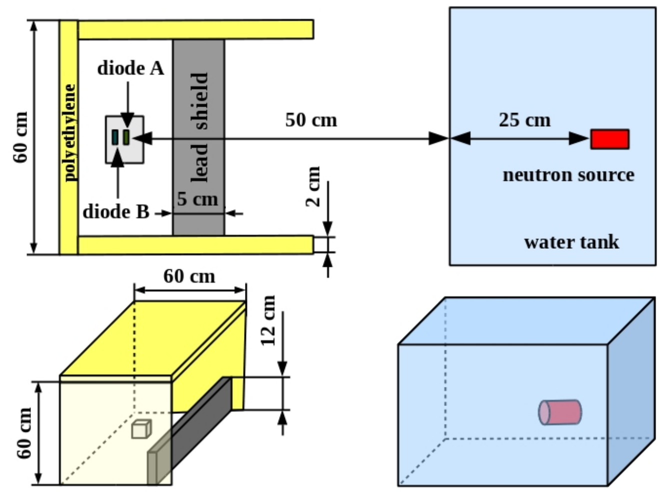


Figure 3: Schematic layout of HDPE experiment.

The predicted value of the total ($\Phi_{t,sim}$) and thermal ($\Phi_{th,sim}$) neutron flux (n/cm$^2$/s) through the 1 cm$^2$ sensitive area of the detector ($^6$LiF film) according to different experimental setups are presented in table 1. Both the values of total and thermal neutron flux are calculated and compared to the real $^{241}$Am-$^9$Be neutron source, which emits $2.5 \times 10^6$ neutron per second (n/s).

Table 1: Thermal ($\Phi_{th,sim}$) and total ($\Phi_{t,sim}$) neutron flux through the surface area of the $^6$LiF film as a function of the different experimental layout.

| Layout (label) | $\Phi_{th,sim}$ (n/cm$^2/s$) | $\Phi_{t,sim}$ (n/cm$^2/s$) | % of $\Phi_{th,sim}$ (Normalised to $\Phi_{t,sim}$) |
|---|---|---|---|
| Basic | 1.9±0.1 | 8.03±0.26 | ≃ 24% |
| HDPE | 7.9±0.2 | 13.1±0.2 | ≃ 60% |

It is apparent from table 1 that, the thermal neutron flux in the “Basic” layout is approximately 24% of the total neutron flux through the converter $^6$LiF film. However, the “HDPE” layout experiment results in a higher thermal neutron flux, which is up to 60% of the total neutron flux through the same converter layer. This is because HDPE sheets facilitate fast neutron thermalisation via elastic collisions between neutrons and hydrogen atoms. Furthermore, the HDPE sheets scatter the thermalised neutrons back to the detector and enhance the field around the converter $^6$LiF film with them. On the other hand, heavy material like lead has minimum effect on the neutron kinetic energy, therefore, lead is ineffective in blocking the incoming neutrons from the source. However, lead works to shield the detector against gamma-rays and reflects the thermal neutrons, which were scattered back from the HDPE sheets towards the detector.

The rate of thermal neutron interaction (dN/dt) is proportional to the number of neutrons crossing the area (A) of the $^6$LiF film of thickness (X).

$$\frac{dN}{dt} = \Phi_{th} \times (AX\Sigma_F) \tag{6}$$

As can be seen from the data in table 1, thermal neutron flux through the $^6$LiF film in the "HDPE" layout experiment is approximately four times the thermal flux in the "Basic" layout experiment. As a result the rate of neutron interaction inside the $^6$LiF film increases by factor 4. This means that on average a neutron will travel through the $^6$LiF film four times and hence is four times more likely to be captured.

$$\left(\frac{dN}{dt}\right)_{HDPE} = 4\left(\frac{dN}{dt}\right)_{Basic} \tag{7}$$

Hence, the probability of thermal neutrons to be captured inside the volume of the sensitive $^6$LiF layer is increased by a factor of 4. In this case the detection efficiency, which has been determined using geant4 simulations can be improved by modifying eq. (**??**) as following

$$\varepsilon = \frac{n}{N} \times P(x) = \frac{n}{N} \times (1 - e^{-4x\Sigma_F}) \tag{8}$$

Consequently, the thermal neutron detection efficiency of one sandwich detector configuration is enhanced by using the HDPE experimental setup.

### 3.2. *Experimental validation of HDPE layout*

The sandwich detector configuration with $^6$LiF film of (1.5±0.6) mg/cm$^2$ thickness has been tested using the HDPE experimental layout (see fig. 3). It has been found that the total and coincidence detection efficiency of one sandwich configuration with such $^6$LiF film thickness increased up to (10.4±0.5)% and (2±1)% respectively as displayed in fig. 4.

The efficiency increases as a result of the effect of the HDPE sheets on the thermal neutrons direction, with the HDPE scattering the neutrons back towards the detector. In addition, these sheets affect the energy and the direction of fast neutrons via the thermalisation process, where fast neutrons are scattered elastically by material such as HDPE, which is rich in light atoms like hydrogen. This process continues until the neutrons are in thermal equilibrium with the surrounding medium, where neutrons cannot lose more energy and they are transferred into thermal neutrons. Hence, the field around the detector is enriched with thermal neutrons and the flux through the converter $^6$LiF film increases as expected from MCNP simulation. This results in increasing the number of neutrons which can be captured by this $^6$LiF film (1.5±0.6) mg/cm$^2$ thick and the thermal neutron detection of the detector is enhanced.

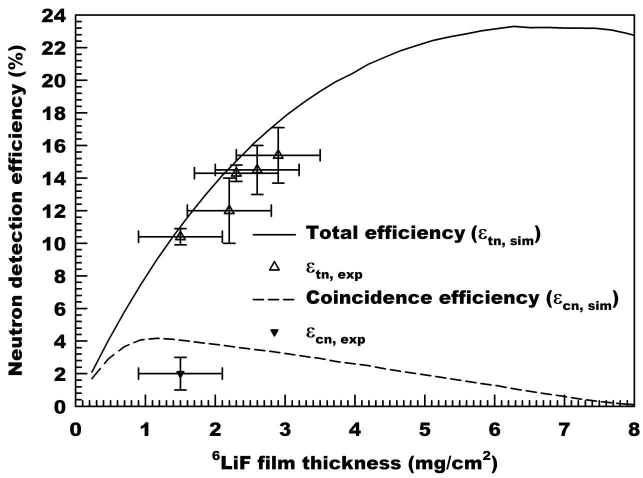


Figure 4: Thermal neutron detection efficiency of the detector as a function of $^6$LiF film thickness corresponding to the HDPE experiment layout.

Another four $^6$LiF films have been prepared and characterised using the same method, which was discussed before, for the purpose of using them in a stacked detector. These films have thicknesses of (2.2±0.6), (2.3±0.6), (2.6±0.6) and (2.9±0.6) mg/cm$^2$. They were tested individually in the "HDPE" experimental layout. The experimental results show that these four $^6$LiF films were able to attain a higher total detection efficiency of (12±2), (14.3±0.5), (14.5±1.5) and (15.4±1.7) respectively. This is due to the increment of $^6$LiF film thickness, which affects and increases the neutron capture probability of the detector. For this reason the detection efficiency increases as the neutron reaction products are still capable of reaching and interacting with Si sensors, specifically the triton particle which has a higher range ($L_t$) through the $^6$LiF film than that of the alpha-particle ($L_\alpha$). The results are in agreement with the predicted behaviour of the total thermal neutron detection efficiency due to the thickness of $^6$LiF film (see fig. 4).

### 3.3. *Advanced stacked detectors design with HDPE*

Stacking individual sandwich detector (Si-$^6$LiF-Si) can increase the overall system neutron detection efficiency. The purpose of the stacking approach is to increase the thermal neutron detection efficiency by increasing the active volume where the neutron can be captured [18]. In this stacked configuration, two coated Si sensors with $^6$LiF films of thicknesses (2.6±0.6) and (2.9±0.6) mg/cm$^2$ have been used with another two bare silicon sensors as a stack of two sandwich detectors. This stack has been mounted in the same aluminium box, which has been used in the previous experiments. The measurements have been

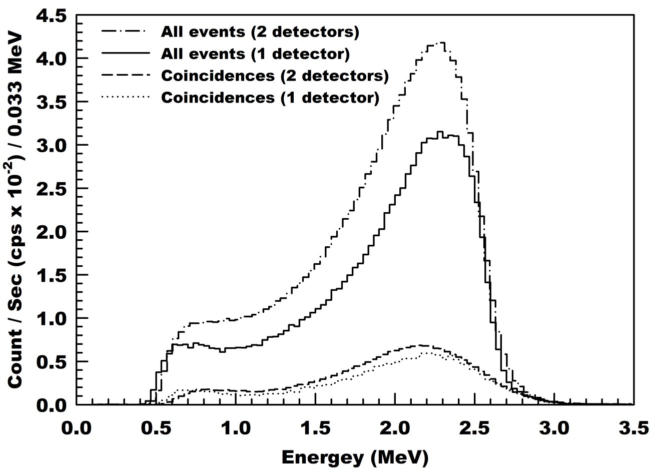


Figure 5: Measured count rate of one and two sandwiches configuration of GAMBE detector with $^6$LiF film in front of $^{241}$Am-$^9$Be neutron source.

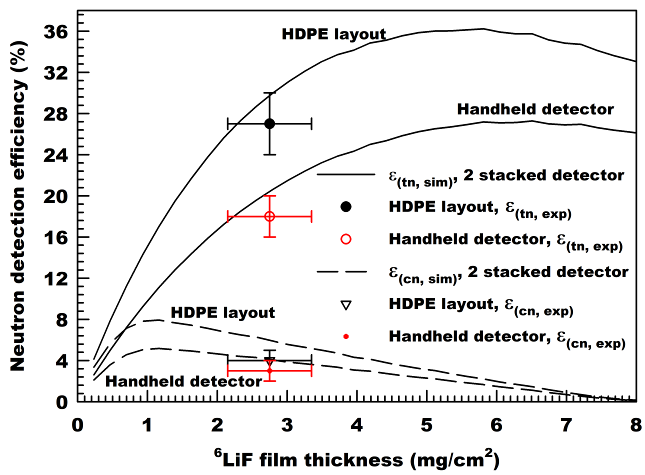


Figure 6: Thermal neutron detection efficiency of the detector as a function of $^6$LiF film thickness corresponding to a stack of two sandwich detectors, which has been tested using the "HDPE" layout and the handheld detector design.

carried out using the "HDPE" layout geometry to examine the thermal neutron detection efficiency of the detector, as a result of the effect of both HDPE sheets and multilayer configuration on the performance of the detector. The stacked detector was able to increase the total and coincidence count rates as it can be seen from the energy spectrum presented in fig. 5.

Consequently, the total and the coincidence detection efficiency was enhanced by about 72% and 47% respectively, comparing to the total and coincidence detection efficiency of (2.9±0.6) mg/cm$^2$ thick $^6$LiF film. This increment of the detection efficiency of the detector is due to the enlargement of the neutron active volume, where the neutrons could be captured. The stack can achieve a total and a coincidence detection efficiency of (27±3)% and (4±1)% respectively, as shown and compared to the results from the simulation in fig. 6. In this figure, the thickness of both $^6$LiF films is considered to be an average thickness of (2.6±0.6) and (2.9±0.6) mg/cm$^2$. The detection efficiency of this stack was not expected to be doubled as a result of neutron attenuation by each $^6$LiF layer, where the neutron flux decreases for each subsequent detector. Moreover, in each reactive layer a proportion of incident neutrons are captured and not all result in a detected event.

### 3.4. Handheld detector configuration

For the purpose of constructing a handheld thermal neutron detector with high thermal neutron detection efficiency. The HDPE experimental layout has been developed into different dimensions, where the lead window (see fig. 3) was replaced by a lead window of 2.5 mm thick and an area of 10 cm × 10 cm. In addition, HDPE sheets were replaced by smaller dimension ones which have the same thickness but different area of 10 cm × 10 cm, where the neutrons can interact and scatter back. It has been found that the total and coincidence detection efficiency of the same stack of two sandwich detectors decreased when the occupied volume by HDPE sheets around the detector was reduced by changing the area of HDPE sheets from 60 × 60 cm$^2$ to 10 × 10 cm$^2$. In this case HDPE sheets work on shielding the detector and scatter thermal neutron away from the detector especially if the neutrons interact with the outer surface of the HDPE box. As a result, the total and the coincidence detection efficiency reduced to (18±2)% and (3±1)% respectively. These results are presented and compared to the predicted performance of the stacked two sandwich detectors corresponding to the handheld detector design (see fig. 6).

The performance of this portable detector can be enhanced by using the available four coated silicon sensors with a $^6$LiF film thickness of (2.2±0.6), (2.3±0.6), (2.6±0.6) and (2.9±0.6) mg/cm$^2$ in a stacked detector of multilayer configuration. Results show that the total detection efficiency of this portable detector raised to (22.8±0.1)% by using these four coated silicon sensors in this stack of two sandwich detectors. However, this modified detector has worse resolution as shown in fig. 7, which will affect $\gamma$/n rejection factor. This is because alpha and triton particles will lose their energy inside each $^6$LiF film before interacting with the sensitive region of the detector. Moreover, the coincidence detection efficiency decreased to a lower level, (0.61±0.02)%, as the alpha particles have been stopped inside the $^6$LiF films, which were on top of each silicon sensor. Therefore, it is suggested that this device works as a counter to detect the presence of thermal neutron detector in the field or for dosimetry purposes.

Finally, simulations suggest that a portable thermal neutron detector can be manufactured using HDPE sheets of thickness 2 cm and dimensions of 10 cm × 10 cm, which will be able to contain a maximum number of 7 sandwich detectors. The design of this handheld thermal neutron detector can achieve a total and a coincidence detection efficiency of 52% and 15% by using an optimal thickness of $^6$LiF film of 3.95 and 0.93 mg/cm$^2$ respectively.

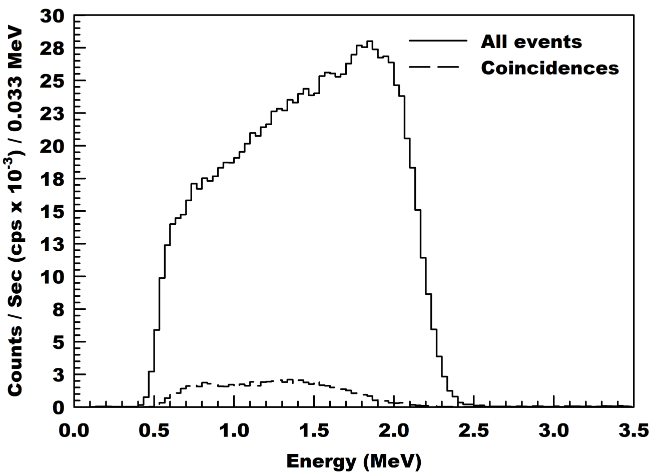


Figure 7: Measured spectrum for $^6$Li(n,$\alpha$)$^3$H reaction products from multilayer configuration of four coated Si sensors with $^6$LiF film.

## 4. Conclusion

The developed neutron detection system, GAMBE, was shown to function effectively as a thermal neutron detector. It has been presented that a detector unit of sandwich configuration with $^6$LiF film of (1.5±0.6) mg/cm$^2$ thick has a total and coincidence detection efficiency of (4.1±0.5)% and (0.9±0.3)% respectively. A method was developed to increase the detection efficiency by using HDPE sheets as a neutron moderator and reflector around the detector to increase the thermal neutron flux through the area of the sensitive $^6$LiF film. As a result of the HDPE sheets the total and the coincidence detection efficiency of one sandwich detector configuration with $^6$LiF film of (1.5±0.6) mg/cm$^2$ thick was enhanced up to (10.4±0.5)% and (2±1)% respectively. The combination of a stacked detector design and HDPE sheets increases the total and coincidence detection efficiency up to (27±3)% and (4±1)% respectively. To study the potential of a handheld detector with a 2.5 mm thick lead window, four coated silicon sensors have been mounted in a stacked design of two sandwich detectors. This portable detector can achieve a high total detection efficiency of (22.8±0.1)% relative to the detection efficiency of $^3$He detector tubes of 1 m long, but this configuration has no significant resolution. In addition, it has been suggested by theoretical investigation that a stack of 7 sandwich detectors for this design will enhance the total and the coincidence detection efficiency up to 52% and 15% respectively.

## References

[1] M. Kelley, Terrorism and the growing threat of weapons of mass destruction: Al-Shabaab, Anchor Academic Publishing (aap_verlag), 2014.

[2] S. Fetter, V. A. Frolov, M. Miller, R. Mozley, O. F. Prilutsky, S. N. Rodionov, R. Z. Sagdeev, Detecting nuclear warheads, Science & Global Security 1 (3-4) (1990) 225–253.

[3] R. Kouzes, E. Siciliano, Alternative neutron detection technology for homeland security, in: APS Meeting Abstracts, Vol. 1, 2009.

[4] R. T. Kouzes, J. Ely, A. T. Lintereur, D. L. Stephens, Neutron detector gamma insensitivity criteria, PNNL–18903, Pacific Northwest National Laboratory, Washington.

[5] R. T. Kouzes, The 3he supply problem, Tech. rep., Pacific Northwest National Laboratory (PNNL), Richland, WA (US) (2009).

[6] D. S. McGregor, H. K. Gersch, J. D. Sanders, R. T. Klann, J. T. Lindsay, Thin-film-coated detectors for neutron detection, Journal of the Korean Association for Radiation Protection 26 (2001) 167–175.

[7] D. S. McGregor, R. Klann, H. Gersch, Y. Yang, Thin-film-coated bulk gaas detectors for thermal and fast neutron measurements, Nuclear Instruments and Methods in Physics Research Section A: Accelerators, Spectrometers, Detectors and Associated Equipment 466 (1) (2001) 126–141.

[8] D. S. McGregor, R. T. Klann, H. K. Gersch, J. D. Sanders, Designs for thin-film-coated semiconductor thermal neutron detectors, in: Nuclear Science Symposium Conference Record (2001 IEEE), Vol. 4, 2001, pp. 2454–2458.

[9] D. S. McGregor, M. Hammig, Y.-H. Yang, H. Gersch, R. Klann, Design considerations for thin film coated semiconductor thermal neutron detectors—i: basics regarding alpha particle emitting neutron reactive films, Nuclear Instruments and Methods in Physics Research Section A: Accelerators, Spectrometers, Detectors and Associated Equipment 500 (1) (2003) 272–308.

[10] G. F. Knoll, Radiation detection and measurement, John Wiley & Sons, 2010.

[11] K. D. Ianakiev, M. T. Swinhoe, A. Favalli, K. Chung, D. W. Macarthur, 6 li foil scintillation sandwich thermal neutron detector, Nuclear Instruments and Methods in Physics Research Section A: Accelerators, Spectrometers, Detectors and Associated Equipment 652 (1) (2011) 417–420.

[12] K. A. Nelson, S. L. Bellinger, B. W. Montag, J. L. Neihart, T. A. Riedel, A. J. Schmidt, D. S. McGregor, Investigation of a lithium foil multi-wire proportional counter for potential 3 he replacement, Nuclear Instruments and Methods in Physics Research Section A: Accelerators, Spectrometers, Detectors and Associated Equipment 669 (2012) 79–84.

[13] J. Allison, K. Amako, J. Apostolakis, H. Araujo, P. A. Dubois, M. Asai, G. Barrand, R. Capra, S. Chauvie, R. Chytracek, G. A. P. Cirrone, G. Cooperman, G. Cosmo, G. Cuttone, G. G. Daquino, M. Donszelmann, M. Dressel, G. Folger, F. Foppiano, J. Generowicz, V. Grichine, S. Guatelli, P. Gumplinger, A. Heikkinen, I. Hrivnacova, A. Howard, S. Incerti, V. Ivanchenko, T. Johnson, F. Jones, T. Koi, R. Kokoulin, M. Kossov, H. Kurashige, V. Lara, S. Larsson, F. Lei, O. Link, F. Longo, M. Maire, A. Mantero, B. Mascialino, I. McLaren, P. M. Lorenzo, K. Minamimoto, K. Murakami, P. Nieminen, L. Pandola, S. Parlati, L. Peralta, J. Perl, A. Pfeiffer, M. G. Pia, A. Ribon, P. Rodrigues, G. Russo, S. Sadilov, G. Santin, T. Sasaki, D. Smith, N. Starkov, S. Tanaka, E. Tcherniaev, B. Tome, A. Trindade, P. Truscott, L. Urban, M. Verderi, A. Walkden, J. P. Wellisch, D. C. Williams, D. Wright, H. Yoshida, Geant4 developments and applications, IEEE Transactions on Nuclear Science 53 (1) (2006) 270–278. doi:10.1109/TNS.2006.869826.

[14] J. F. Briesmeister, et al., Mcnptm-a general monte carlo n-particle transport code, Version 4C, LA-13709-M, Los Alamos National Laboratory (2000) 2.

[15] C. Leroy, P.-G. Rancoita, Principles of radiation interaction in matter and detection, Vol. 2, World Scientific, 2009.

[16] M. Gomaa, B. Henaish, E. Ali, Calculated neutron and gamma dose rates around a moderated am-be neutron source, Applied Radiation and Isotopes 44 (3) (1993) 638–640.

[17] S. Srivastava, R. Henry, A. Topka, Characterization of pin diode silicon radiation detector, Journal on Intelligent Electronic Systems 1 (1) (2007) 48.

[18] D. Moses, Efficient scalable solid-state neutron detector, Review of Scientific Instruments 86 (6) (2015) 065103.